J. Phys. A: Math. Gen. **33** (2000) 1809–1825. Printed in the UK PII: S0305-4470(00)02416-1

Topological invariants in period-doubling cascades

C Letellier, S Meunier-Guttin-Cluzel and G Gouesbet

LESP—CORIA UMR 6614—Université et INSA de Rouen, Place Emile Blondel, 76131 Mont-Saint-Aignan, France

Received 8 March 1999, in final form 8 September 1999

Abstract. Topological characterization is a useful description of dynamical behaviours as exemplified by templates which synthesize the topological properties of very dissipative chaotic attractors embedded in tri-dimensional phase spaces. Such a description relies on topological invariants such as linking numbers between two periodic orbits which may be viewed as knots. These invariants may, therefore, be used to understand the structure of dynamical behaviours. Nevertheless, as an example, the celebrated period-doubling cascade is usually investigated by using total twists which are not topological invariants. Instead, we introduce linking numbers between an orbit, viewed as the core of a small ribbon, and the edges of the ribbon. Such a linking number (which is in fact the Cãlugãreanu invariant) is related to the total twist number and the number of writhes of the ribbon. A second topological invariant, called the effective twist number, is also introduced and is useful for investigating period-doubling cascades. In the case of a trivial suspension of a horseshoe map, this topological invariant may be predicted from a symbolic dynamics with the aid of framed braid representations.

1. Introduction

A deep knowledge of dynamical systems may be gained by using the topological properties of the associated phase portraits. Since a chaotic attractor is built on a skeleton of periodic orbits, this issue may be reduced to the study of the relative organization of periodic orbits. Starting from the fact that a periodic orbit is a closed loop, it may be viewed as a knot and, consequently, the knot theory may be used to describe the structure of the dynamics. This is, however, restricted to the case when the phase portrait is embedded in a tri-dimensional space since when the dimension is higher, all knots are trivial and all links are unlinked. In this framework, Birman and Williams [1, 2] introduced a branched surface called a template, on which all periodic orbits embedded within the attractor may be projected. A template allows one to predict the linking numbers between pairs of periodic orbits [3–6]. Actually, the linking-number concept is the relevant one used in this approach. A linking number is a topological invariant, i.e. it is preserved under an ambient isotopy which relates a knot to another one by a continuous deformation through embeddings. From a dynamical point of view, such an invariant is therefore robust since it is not affected by a modification of the control parameters when the involved periodic orbits are not implied in a bifurcation.

However, period-doubling cascades are usually investigated in terms of rotation numbers of eigenvectors along periodic orbits [7], or of relative rotation numbers of other quantities listed in [8]. The number of half-turns of the small ribbon generated by the end of one of the eigenvectors is the so-called *total twist* number τ. Unfortunately, this number is not a topological invariant. Instead, it is then desirable to use a topological invariant (preferably easy to compute) to topologically describe period-doubling cascades (or other dynamical

0305-4470/00/091809+17$30.00

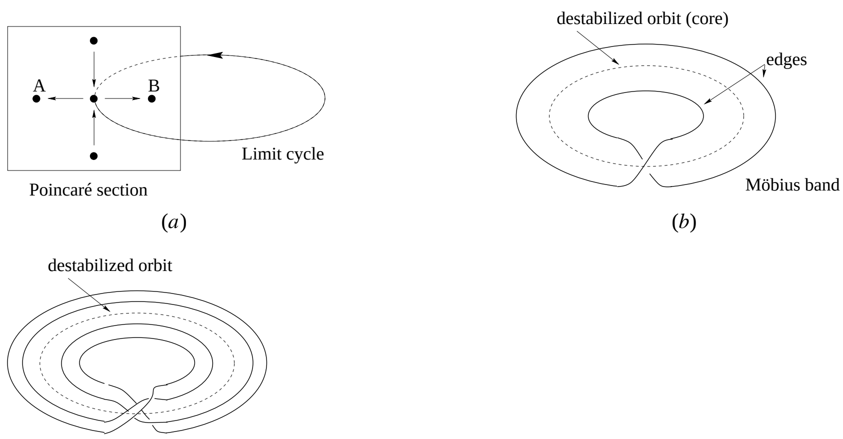

(*a*) (*b*)

(*c*)

Figure 1. Topological structure of manifolds after bifurcations. (*a*) Local analysis of the bifurcation. (*b*) Manifolds of the destabilized orbit after the bifurcation. (*c*) Manifolds of the newly born orbit.

behaviours). In this paper, we then stress the interest of using (appropriately defined) linking numbers and effective twist numbers rather than total twist. Effective twist numbers are numbers defined as being the sum of the number of half-turns performed by the ribbon rotating around its core (the orbit) plus twice the number of writhes.

This paper is organized as follows. In section 2 we present a concise description of the mechanisms involved in a period-doubling cascade in terms of rotation numbers and symbolic dynamics. Section 3 is devoted to the analysis of topological properties by using linking numbers between an orbit, viewed as the core of a ribbon, and the edges of the ribbon. Section 4 explains how these linking numbers may be predicted from symbolic dynamics and how rotation numbers may be predicted in the case of a trivial suspension of a horseshoe map. Section 5 concludes the paper.

2. Period-doubling structures

In a period-doubling bifurcation, a limit cycle is destabilized to a new limit cycle whose period is twice the original period. The nature of the bifurcation may also be exhibited by using a Poincaré section in the neighbourhood of the original limit cycle. At the bifurcation, the characteristic multiplier is exactly equal to (-1). Slightly after the bifurcation, the characteristic multiplier is real and negative. The first-return map to a Poincaré section then takes a point A to a point B, as depicted in figure 1(*a*) with points A and B located alternatively with respect to the original periodic point. In the most simple case, the manifolds of the destabilized orbit undergo one half-revolution around it. Each manifold then locally lies on a Möbius band with only one side and one edge (figure 1(*b*)), generating a strip whose topology is unchanged up to the next bifurcation involving this periodic orbit. More generally, after a period-doubling bifurcation, each manifold of the destabilized orbit necessarily rotates an odd number τ of half-turns per cycle.

After the bifurcation, a new periodic orbit is born. The ribbon associated with this newly born stable orbit may be obtained by splitting the Möbius band displayed in figure 1(*b*) along the core (the destabilized orbit). This process generates a ribbon with an even number of

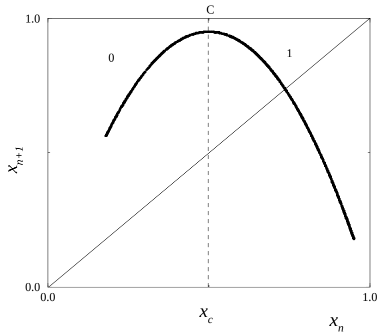

Figure 2. Generating partition of the logistic map induced by its differentiable maximum C ($\mu = 3.8$).

half-turns, i.e. with two sides and two edges (figure 1(c)). Manifolds of the newly born orbit whose period is twice the period of the destabilized orbit then undergo an even number of half-turns. Since a manifold of a stable orbit must undergo an odd number of half-turns to allow a destabilization of the orbit by a period-doubling bifurcation, as required by the characteristic multiplier being equal to (-1) at the bifurcation, manifolds have to topologically evolve when a control parameter is varied to the next bifurcation. More specifically, one half-turn has to be added or deleted before the occurrence of a new period-doubling bifurcation. Such a local description is quite useful to understand the mechanism of the period-doubling cascade and explains why many investigations of period-doubling cascades are achieved by using the number of half-turns τ, i.e. the total twist number [7, 9–11].

Another useful tool to describe a period-doubling cascade, and more generally any kind of bifurcation, is the symbolic dynamics. Let us introduce it in the simple case of the logistic map. The logistic map is a unimodal map with a differentiable maximum

$$x_{n+1} = f(x_n) = \mu x_n (1 - x_n). \tag{1}$$

This map is associated with a horseshoe dynamics. It may be viewed as a first-return map to a Poincaré section of a flow, and is constituted by an increasing monotonic branch and by a decreasing monotonic branch separated by a *critical point* C at the maximum of the map (figure 2) with coordinate x_c. This critical point induces a generating partition which allows one to encode all trajectories $\{x_n\}$ by a string of symbols $\sigma_0\sigma_1\sigma_2 \ldots \sigma_n \ldots$, where

$$\sigma_n = \left| \begin{array}{lll} 0 & \text{if} & x_n < x_c \\ 1 & \text{if} & x_n > x_c \end{array} \right. \tag{2}$$

except the orbit associated with the iteration of the critical point C. When a suspension of a unimodal map (or equivalently a horseshoe map) is considered, it may be shown that the increasing branch is associated with a strip with an even number of half-turns and the decreasing branch with a strip with an odd number of half-turns [12].

Rigorously, the aforementioned symbolic dynamics may be used for control parameter values for which the invariant set is hyperbolic. In practice, a periodic orbit may be encoded by a string corresponding to control parameter values for which the orbit is unstable. When a period-p orbit is born at the very moment of a bifurcation, it is associated with a string, such that

$$x_1 = f(x_c) \qquad x_2 = f^2(x_c), \ldots, x_p = f^p(x_c) = x_c \tag{3}$$

where x_c is the coordinate of the critical point C and the function f denotes the map. More generally, a string $\{\sigma_n\} = \sigma_1\sigma_2 \ldots \sigma_p$ is used to encode a period-p orbit (among the other

$(p - 1)$ cyclic permutations). For instance, the period-4 orbit generated after two period-doubling bifurcations is encoded by using the string $\sigma_1\sigma_2\sigma_3\sigma_4$ which corresponds to the symbolic sequence (1011).

Let us now briefly describe how a period-doubling cascade is encoded starting from the period-2 orbit. This orbit is encoded on $\Sigma_2 = \{0, 1\}$ as (10) after its birth. Just after the next bifurcation, its daughter is encoded by 1010, i.e. the symbolic sequence of the mother is repeated twice. One may then remark that the orbit is encoded by an even sequence, i.e. with an even number of 1s, each 1 being associated with a strip whose total twist is odd (the number of 0s is irrelevant since each 0 is associated with a strip whose total twist is even). This process corresponds to the mechanism previously described. The newly born period-4 limit cycle is associated with a stable manifold which has to evolve until it exhibits an odd number of half-turns, a condition which is compulsory to allow a new period-doubling bifurcation. This evolution is associated with a periodic point (x_p according to our convention) which passes from one monotonic branch to the other, via the critical point C, leading to the following symbolic representation:

$$1010 \rightarrow 101\mathrm{C} \rightarrow 1011. \tag{4}$$

It may then be readily checked that the orbit 1011 (with an odd number of 1s) lies on a ribbon rotating an odd number of half-turns around it. If n is the order of the bifurcation involved in the cascade, the number of half-turns generated by passing the critical point is $(-1)^n$, as exhibited by the following encoding of the period-doubling cascade:

$$\begin{array}{cc} (1) & n = 0 \\ (10) \leftarrow 1\mathrm{C} \leftarrow 11 & n = 1 \\ 1010 \rightarrow 101\mathrm{C} \rightarrow (1011) & n = 2 \\ (1011\ 1010) \leftarrow 1011\ 101\mathrm{C} \leftarrow 1011\ 1011 & n = 3 \\ \vdots & \end{array} \tag{5}$$

After the accumulation point of the cascade, no other period-doubling bifurcation is possible. Then, a saddle-node bifurcation creates a pair of periodic orbits. One of them is unstable and lies on a ribbon with an even number of half-turns and the other is stable. The latter one is thereafter destabilized by a new period-doubling bifurcation generating a new cascade. As a consequence, in a pair of periodic orbits created by a saddle-node bifurcation, one is encoded by an even symbolic sequence and the other by an odd symbolic sequence. For instance, there exists a pair of period-5 orbits involved in a saddle-node bifurcation encoded by (10111) and (10110). The second one, having an odd number of 1s, may then induce a period-doubling cascade. The number of half-turns of the ribbons associated with each orbit in such a pair differs by ± 1. The unstable periodic orbit (10111) is a *regular saddle* also called the father and the stable one (10110) is a *flip saddle* called the mother. The mother will have a daughter encoded (10110 10111) generated by a period-doubling bifurcation.

3. Linking numbers

Investigating topological properties should preferably rely on topological invariants which do not depend on the diagrammatic representation used. Unfortunately, the total twist τ is not a topological invariant since it is not preserved under an ambient isotopy. This fact is exemplified in figure 3 where a ribbon with a writhe and no half-turn (figure 3(*a*)) is isotopically changed to a ribbon without any writhe but with a full twist (figure 3(*b*)) having a total twist equal to -2 (expressed in terms of half-turns). Letting L_α (resp. L_β) be the link constituted by the edges

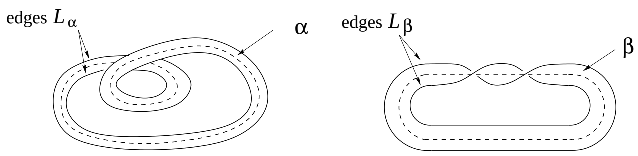

Figure 3. Exchanging a writhe for a full twist under an isotopy. The periodic orbit α (resp. β) is the core of the ribbon defined by the link formed by the edges L_α (resp. L_β). Ribbons defined by edges L_α and L_β are topologically equivalent. (*a*) A writhe and (*b*) a full twist.

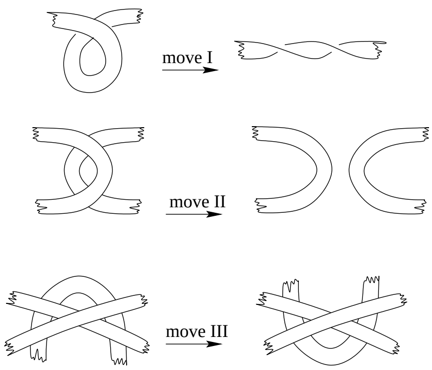

Figure 4. Ambient isotopy of ribbons by using Reidemeister moves. Move I changes a writhe to a full twist. These moves are reversible.

of the ribbon, whose orbit α (resp. β) is the core, we have

$$\begin{aligned} \tau(L_\alpha) = 0 \qquad &\text{and} \qquad \omega(L_\alpha) = -1 \\ \tau(L_\beta) = -2 \qquad &\text{and} \qquad \omega(L_\beta) = 0 \end{aligned} \tag{6}$$

where $\tau(L_\alpha)$ and $\tau(L_\beta)$ are the number of oriented half-turns and $\omega(L_\alpha)$ and $\omega(L_\beta)$ are the number of oriented writhes according to the convention:

(7)

As for knots, we may introduce Reidemeister moves for ribbons displayed in figure 4. Note that the Reidemeister moves of type-II and type-III on the cores of the ribbons extend to the ribbons themselves. Such a correspondence between the core and the ribbon does not exist for the type-I move. Instead, a type-I move on the core generates a full twist on the ribbon.

Although move I implies that the total twist $\tau(L_\alpha)$ is not a topological invariant, we see that the sum of twice the number of writhes and the total twist defines a quantity which is invariant under an isotopy. We, however, have two cases to consider depending on whether the edges form a two-component link (as in figure 3) or a knot (as in figure 1(*b*)).

In the case of a regular saddle, the ribbon has two distinct edges which define a 2-component link L_α. For an appropriate class of 2-component link made out of half-turns and writhes associated with a core which may be reduced to a trivial knot by using Reidemeister moves, a linking number $lk(L_\alpha)$ between the two components of the link may then be defined according to

$$lk(L_\alpha) = 2\omega(L_\alpha) + \tau(L_\alpha) \tag{8}$$

where $\tau(L_\alpha)$ is the total twist of L_α and $\omega(L_\alpha)$ is the number of writhes of L_α [13]. The relation is slightly different here from the one used by Kauffman because the number of twists is counted in terms of half-turns rather than in terms of full-turns. In the case of the topologically equivalent links L_α and L_β displayed in figure 3, we then have $lk(L_\alpha) = lk(L_\beta) = -2$. In fact, this linking number is equal to the Călugăreanu invariant [14] whose review is given in [15]. The number of writhes $\omega(L_\alpha)$ may be estimated by using the self-linking number $slk(\alpha)$ of the core α which is defined as the algebraic sum of crossings on the core α [15]. Note that the self-linking number $slk(\alpha)$ is expressed in terms of full-turns. Since the writhe number is expressed in terms of full-turns, we have $\omega(Ł_\alpha) = slk(\alpha)$. Relation (8) may then be rewritten as

$$lk(L_\alpha) = 2slk(\alpha) + \tau(L_\alpha). \tag{9}$$

The self-linking number may be rewritten as

$$slk(\alpha) = slk(\alpha^R) + \omega_R(L_\alpha) \tag{10}$$

where α^R is the minimal diagrammatic representation of the core α, i.e. with the smallest number of crossings, and $\omega_R(L_\alpha)$ is the number of writhes vanished by moves I in the reduction of the core α to its minimal representation α^R.

However, the linking number $lk(\alpha)$ is useless when the edges form a knot as in figure 1. This leads us to the introduction of another topological invariant. Postponing the case when the edges form a knot, let us first introduce this topological invariant in the case when the edges form a two-component link. Let the link L_α consist of two edges E_1 and E_2. We then define the topological invariant $\tilde{lk}(L_\alpha, \alpha)$ as the sum of the two linking numbers $lk(E_1, \alpha)$ and $lk(E_2, \alpha)$, each one being the linking number between the core α and one of the edges of the associated ribbon, according to

$$\tilde{lk}(L_\alpha, \alpha) = lk(E_1, \alpha) + lk(E_2, \alpha). \tag{11}$$

We call $\tilde{lk}(L_\alpha, \alpha)$ a *quasi-linking number*. It is an invariant because it is the sum of two invariants. For orbits α and β displayed in figure 3, we have $\tilde{lk}(L_\alpha, \alpha) = \tilde{lk}(L_\beta, \beta) = lk(L_\alpha) = -2$. This quasi-linking number $\tilde{lk}(L_\alpha, \alpha)$ also reads as

$$\tilde{lk}(L_\alpha, \alpha) = \frac{1}{2} \sum_{c \in L_\alpha \sqcap \alpha} \epsilon(c) \tag{12}$$

where $c \in L_\alpha \sqcap \alpha$ designates the crossings between the core α and the two components of L_α, self-crossings being ignored. Also, $\epsilon(c)$ is the sign of the crossing c with the usual convention, i.e.

ε=+1 ε=−1 (13)

As for the usual linking number $lk(\alpha, \beta)$ of two oriented knots α and β, the quasi-linking number $\tilde{lk}(L_\alpha, \alpha)$ gives an intuitive notion of how many times the ribbon defined by the link L_α winds around α. Also, the quasi-linking number $\tilde{lk}(L_\alpha, \alpha)$ is expressed in terms of half-turns involved in equation (8) to allow a description of Möbius bands by using integers.

Indeed, when a flip saddle is considered, the associated ribbon is a Möbius band and has a single edge. Therefore, the edges L_α now generate a knot instead of a two-component link. For large periodic orbits, the quasi-linking number $\tilde{lk}(L_\alpha, \alpha)$ is still defined as the sum of linking numbers between α and the components E_i formed by the edges, as in the case of regular saddles. However, since the edges form only one component, the quasi-linking number $\tilde{lk}(L_\alpha, \alpha)$ now reduces to an usual linking number defined between two knots in contrast with the case of regular saddles where three knots are involved. As we see, an essential advantage of

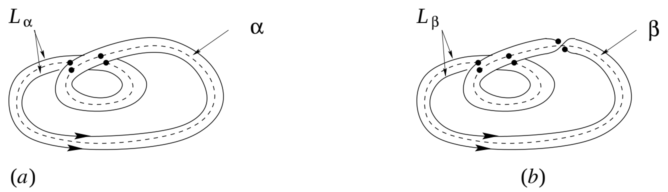

Figure 5. A pair of periodic orbits α and β which could be created by a saddle-node bifurcation, where ● designate negative crossings. (*a*) The regular saddle: $\tilde{lk}(L_\alpha, \alpha) = \frac{1}{2}(-4) = -2$. (*b*) The flip saddle: $lk(L_\beta, \beta) = \frac{1}{2}(-6) = -3$.

using $\tilde{lk}(L_\alpha, \alpha)$ is then that it is defined in the same way for regular and flip saddles, providing a topological invariant of the same nature for both saddles. An example of a pair of periodic orbits appearing in a saddle-node bifurcation is displayed in figure 5. The quasi-linking number $\tilde{lk}(L_\alpha, \alpha)$ for the regular saddle and the linking number $lk(L_\beta, \beta)$ for the flip saddle differ by ± 1, a feature which is characteristic of such an orbit pair. Since each self-crossing of the core α is associated with four crossings between edges L_α and the core α, the quasi-linking numbers may be rewritten as

$$\tilde{lk}(L_\alpha, \alpha) = 2slk(\alpha) + \tau(L_\alpha) \tag{14}$$

which is in agreement with relation (12).

More generally, by using the quasi-linking number $\tilde{lk}(L_\alpha, \alpha)$ between an orbit α and the edges L_α of the ribbon whose orbit α is the core, any periodic orbit may be topologically characterized in any situation. In what follows, the terminology 'linking number'is preferred when the quasi-linking number reduces to a linking number in the strict sense.

4. Predicting linking numbers with a symbolic dynamics

The quasi-linking numbers $\tilde{lk}(L_\alpha, \alpha)$ may be predicted from the symbolic sequence of the core α, by using the algebraic evaluation of linking numbers introduced in [17]. With this procedure, the self-linking numbers may be predicted from the symbolic sequence of the orbit considered and from the linking matrix describing the template of the attractor. The linking matrix is a square matrix $k \times k$, where k is the number of monotonic branches exhibited on a first-return map. Its elements M_{ij} are defined as follows. M_{ii} designates the number of half-turns in the ith branch of the template and M_{ij} is the sum of oriented crossings between the ith and the jth branches ($i \neq j$) [16]. Let us start by predicting the self-linking number $slk(\alpha)$ where α is a period-p orbit encoded by $(\sigma_1 \ldots \sigma_p)$ on a set of symbols. In the case considered here, $k = 2$. According to the algebraic evaluation proposed in [17], self-linking numbers read as

$$slk(\alpha) = N_{\text{lay}}(\alpha) + \left[\sum_{i,j} M_{\sigma_i \sigma_j} \right]_{i \neq j} \tag{15}$$

where $N_{\text{lay}}(\alpha)$ is the layering crossing number counted on the layering graph of the template (see figure 2 of [17]). The total twist $\tau(L_\alpha)$ is equal to the number of half-turns induced by the total twist of the branches of the template (see figure 2 in [17]). Indeed, when a segment of the considered orbit passes a branch with half-turns, the ribbon associated with this orbit also presents these half-turns. Consequently, the total twist $\tau(L_\alpha)$ is given by

$$\tau(L_\alpha) = \sum_{i=1}^{p} M_{\sigma_i \sigma_i}. \tag{16}$$

Table 1. Quasi-linking numbers $\tilde{lk}(L_{\alpha_n}, \alpha_n)$ for saddles involved in two period-doubling cascades. See the main text for the other numbers also reported. α_n must be replaced by β when the regular saddle is considered. In particular, $\tau(L_{\alpha_n})$ appears in equation (25) and $(p_n - q_n)$ in equation (26).

Saddle	n	$\tilde{lk}(L_{\alpha_n}, \alpha_n)$	$slk(\alpha_n)$	$\tau(L_{\alpha_n})$	$(p_n - q_n)$	$slk(\alpha_n^R)$	$T(L_{\alpha_n})$
(0)	regular	0	0	0	0	0	0
(1)	0	1	0	1	0	0	1
(10)	1	3	1	1	1	0	3
(1011)	2	13	5	3	2	3	7
	3	51	23	5	4	19	13
	4	205	97	11	8	89	27
	5	819	399	21	16	383	53
(101)	regular	6	2	2	2	0	6
(100)	0	5	2	1	2	0	5
(100101)	1	21	9	3	4	5	11
	2	83	39	5	8	31	21
	3	333	161	11	16	145	43
	4	1331	655	21	32	623	85
	5	5325	2641	43	64	2577	171

According to relation (14), the quasi-linking numbers then read as

$$\tilde{lk}(L_\alpha, \alpha) = 2\left(N_{\text{lay}}(\alpha) + \left[\sum_{i,j} M_{\sigma_i\sigma_j}\right]_{i\neq j}\right) + \sum_{i=1}^{p} M_{\sigma_i\sigma_i}. \tag{17}$$

The quasi-linking numbers may then be predicted with a symbolic dynamics and a linking matrix (nevertheless, an algorithm implemented on a computer is required for large periodic orbits). They are reported in table 1 in the case of the trivial suspension of a horseshoe map corresponding to a template characterized by a linking matrix [16]

$$\begin{bmatrix} 0 & 0 \\ 0 & +1 \end{bmatrix}. \tag{18}$$

In table 1, the subscript n recalls the order of the period-doubling bifurcation in the cascade induced by the flip saddle α_0 which has been created by a saddle-node bifurcation with a regular saddle β. Orbits α_0 and β have a same period p. Thus, after the nth bifurcation, the newly born orbit has a period equal to $(2^n \times p)$. For instance, the orbit characterized by $(p = 3, n = 2)$ arises from the cascade

$$\begin{array}{lll} S_\beta = (101) & S_{\alpha_0} = (100) & n = 0 \\ S_{\alpha_1} = (100\ 101) & & n = 1 \\ S_{\alpha_2} = (100\ 101\ 100\ 100) & & n = 2 \end{array} \tag{19}$$

where S_i is the symbolic sequence corresponding to the orbit i. The quasi-linking numbers and the self-linking numbers are computed by using an algorithm implemented on a computer involving the symbolic dynamics and the linking matrix of the template. The code detects each oriented crossing on the template construction (explicit relationships have also been demonstrated as reported in appendix A).

From table 1, one may remark that the quasi-linking numbers obey the recurrence law

$$\tilde{lk}(L_{\alpha_{n+1}}, \alpha_{n+1}) = 4\tilde{lk}(L_{\alpha_n}, \alpha_n) + (-1)^m \tag{20}$$

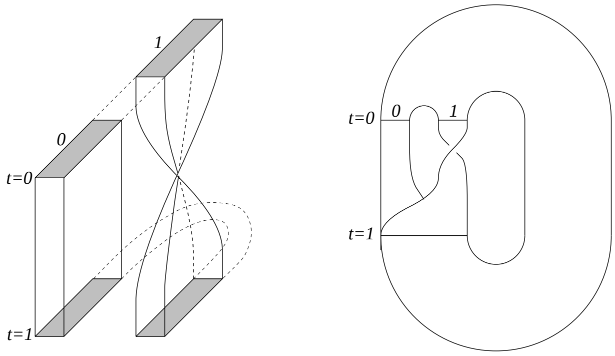

Figure 6. The trivial flow as a suspension of a horseshoe map.

with

$$\left| \begin{array}{ll} m = n & \text{if} \quad lk(L_{\alpha_0}, \alpha_0) < \tilde{lk}(L_\beta, \beta) \\ m = n + 1 & \text{if} \quad lk(L_{\alpha_0}, \alpha_0) > \tilde{lk}(L_\beta, \beta) \end{array} \right. \tag{21}$$

where α_0 designates the flip saddle and β the regular saddle, both created in a saddle-node bifurcation. It must be remarked that there is one exception. Indeed, this relation is valid for all period-doubling bifurcations except in the case where $n < 2$ for $p = 1$.

The total twist $\tau(L_{\alpha_n})$ obeys a recurrence law

$$\tau(L_{\alpha_{n+1}}) = 2\tau(L_{\alpha_n}) + (-1)^m. \tag{22}$$

Using this number, a recurrence rule may also be exhibited for the self-linking number $slk(\alpha_n)$:

$$slk(\alpha_{n+1}) = 4slk(\alpha_n) + \tau(L_{\alpha_n}) \tag{23}$$

which is, in fact, the one proposed by [8].

In the remaing part of this section, we limit ourselves to the case of a horseshoe map

$$x_{n+1} = g_\mu(x_n) \tag{24}$$

which may be akin to a Poincaré map on a planar section of a flow. This may be viewed by choosing the simplest embedding of the suspension of g, yielding a flow connecting points at time $t = 0$ and $t = 1$ with a trivial flow as displayed in figure 6. By trivial flow, we mean a suspension of the horseshoe map without any global torsion, i.e. without any twist on the unbranched part of the template.

Henceforth, we refer to this as the natural suspension of g. This suspension creates a flow, generating periodic orbits of infinitely many knot types.

It has been shown that it is possible to directly predict the quasi-linking number $\tilde{lk}(L_\alpha, \alpha)$ from a symbolic dynamics. Another useful topological invariant may also be computed. It counts the number of half-turns the ribbon locally rotates arount its core α when this latter is reduced to its minimal representation α^R (this reduction annihilates the writhes). This number, designated by $T(L_\alpha)$ and here called the effective twist number, is therefore equal to

$$T(L_\alpha) = \omega_R(L_\alpha) + \tau(L_\alpha) \tag{25}$$

where $\omega_R(L_\alpha)$ is the number of writhes vanished by move I in the reduction of the core α to its minimal representation α^R. Obviously, we have $T(L_\alpha) = T(L_\alpha^R)$. This number is reported in table 1 as well as the self-linking number $slk(\alpha^R)$ of the minimal diagrammatic representation of the core α. $\omega_R(L_\alpha)$ is, therefore, equal to $slk(\alpha) - slk(\alpha^R)$. Both of them may be predicted from symbolic dynamics by using the concept of framed braid (even if the self-linking numbers

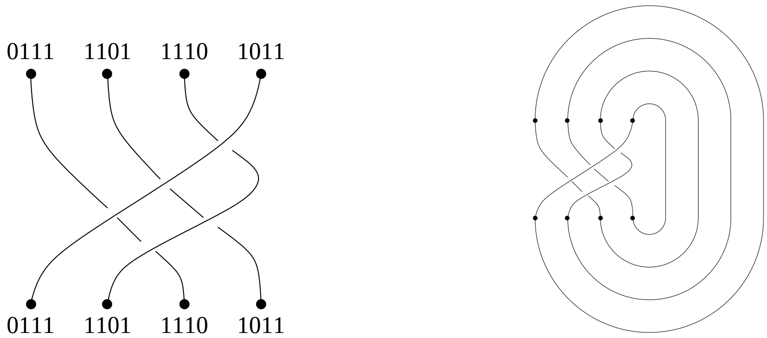

(*a*) Braid (*b*) Closed braid

Figure 7. Periodic orbit (1011) represented as a braid. The periodic points on the base lines are ordered following the unimodal order. Connections between upper base points and lower base points are drawn from the template construction (all crossings are positive).

may be only hand-predicted for low periodic orbits and, consequently, an implementation of the algorithm on a computer is required).

A braid is a regular representation of a link in which all strands travel monotically along an axis. There is a theorem due to Alexander [18] according to which all knots and links can be represented in such a fashion. The set of all braids on p strands has a group structure associated with it: the braid group. For further details, see Ghrist and Holmes [19]. A positive braid is one for which all crossings are positive as it occurs in the case of the periodic orbits generated by the template displayed in figure 6.

To obtain a standard representation of a given periodic orbit generated by the horseshoe template, the kneading theory may be used. All periodic points may then be ordered according to the unimodal order to constitute the two horizontal base lines between which a geometric braid is built in agreement with the horseshoe template. From upper base points, we draw p strands to the lower base points by connecting a symbolic sequence to its first cyclic permutation, following the template construction (figure 7). By connecting opposite ends of the strands, in the standard way, we form a closed braid. Each closed braid is a knot or a link.

The twisted structure of the periodic orbits in a braid may be exhibited by using framed braids as explained by Tufillaro *et al* and Melvin and Tufillaro [5, 16]. A framed braid is a braid with a positive or negative integer associated with each strand. This integer is called the total *torsion* (of the strand) representing an internal structure of the strand. For instance, if each strand is a physical cable, then we could subject this cable to a torsion force causing a twist. In the present instance, the total torsion would represent the number of half-turns in the cable.

Geometrically, a framed braid can be represented by a ribbon graph. Take a braid diagram as displayed in figure 8(*a*) and replace each strand by a ribbon (figure 8(*b*)). To represent the torsions, we twist each ribbon by an integer number of half-turns. We will use these framed braids as a useful representation to reduce the periodic orbits to their minimal knot diagrams taking into account the torsion of the ribbon whose orbit is the core.

Noting that move II and move III do not change the framing of implied strands and that move I induces a variation of ± 2 (+2 for a positive braid as here) of the framing, depending on the sign of the writhe (figure 9), we simplify the periodic orbits as exemplified in the case of the orbit (1011) displayed in figure 10. After a simplification, a number of half-turns, equal

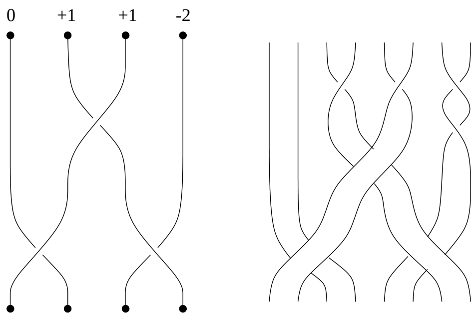

(a) Framed braid (b) Ribbon graph

Figure 8. Geometric representation of a framed braid as a ribbon graph. The integer attached to each strand is the sum of the half-turns in the corresponding branch of the ribbon graph (adapted from Tufillaro *et al* [5]).

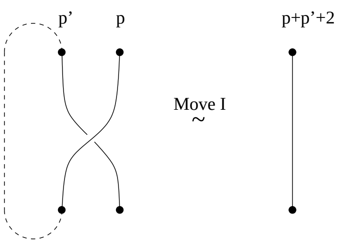

Figure 9. Reduction of the number of strands by using a move I changing a writhe to a full twist.

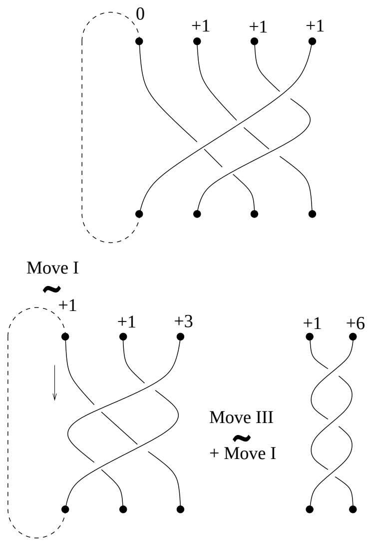

Figure 10. Reduction of the period-4 orbit (1011) by using Reidemeister moves. The framed braid is used to give a schematic view of this process. The number $T(1011^R)$ is found to be equal to +7 as reported in table 2 ($p = 1, n = 2$).

to the sum of the framing of each strand, is exhibited: it corresponds to the effective twist number $T(L_\alpha)$ of the orbit α.

By using the Reidemeister moves, the orbit diagram has been simplified to a minimal diagram. Its corresponding framed braid has two strands. This minimal number of strands is an invariant which is called the *braid index* [19]. Given a braid β, the braid index $b(\beta)$ is the smallest integer q such that β has a presentation as a braid on q strands. The braid index is usually different from the dynamical period p of a given period-p orbit which is a dynamical invariant, though not an isotopy invariant.

Ghrist and Holmes [19] demonstrated that the braid index may directly be obtained from the symbolic dynamics. Given a knot encoded by a word

$$S = 0^{n_1}1^{m_1}0^{n_2}1^{m_2}\dots0^{n_k}1^{m_k}$$

syllables are defined to be of the form 0^n1, 0^n1^2 and 1^2, for arbitrary $n > 0$. Then each word (except the trivial words 0–1) has a unique decomposition into such syllables and each syllable in the word corresponds to a single strand on the well disposed braided template.

Proposition. *The braid index of a horseshoe knot K is equal to the number of syllables in S.*

For instance, the orbit (1011) may be decomposed in two syllables 01 and 1^2:

$$0111 \equiv 01 \cdot 1^2.$$

Its braid index $b(1011)$ is therefore equal to 2 as displayed in figure 10. The case of orbit (1011 1010) is given in appendix B. Up to now, the prediction of quasi-linking numbers $\tilde{lk}(L_\alpha, \alpha)$ is limited to the special case of a trivial suspension of a horseshoe map since the proposition is only valid in this case.

One may remark that each time a strand is removed, a move I is implied exchanging a writhe to a full-twist. From equation (25), it is then found that the effective twist number $T(L_\alpha)$ exhibited on the simplified framed braid of a period-p orbit α is given by

$$T(L_\alpha) = 2(p - q) + \tau(L_\alpha) \qquad (26)$$

where q is equal to the braid index. The effective twist numbers $T(L_\alpha)$ may therefore be predicted by using the symbolic dynamics. Effective twist numbers $T(L_\alpha)$ are reported in table 2 in the case of a trivial suspension of a horseshoe map.

In order to distinguish orbits created in a cascade generated by different pairs of saddles whose period are equal, we introduce a subscript which indicates their relative order according to the unimodal order. For instance, the pair ($S_\beta = (10111)$, $S_{\alpha_0} = (10110)$), associated with $p = 5_1$ appears before the pair ($S_\beta = (10010)$, $S_{\alpha_0} = (10011)$), associated with $p = 5_2$.

By inspecting table 2, one may check that the effective twist numbers $T(L_\alpha)$ satisfy a recurrence relationship (excepted for $p = 1, n = 1$):

$$T(L_{\alpha_{n+1}}) = 2T(L_{\alpha_n}) + (-1)^m. \qquad (27)$$

From (27), a second rule may be derived, reading as

$$T(L_{\alpha_{n+2}}) = 2T(L_{\alpha_n}) + T(L_{\alpha_{n+1}}). \qquad (28)$$

The origin of the recurrence relationship (28) may then be exhibited by the symbolic sequences since all periodic orbits implied in a period-doubling cascade are encoded by a word of the form

$$S_{n+1} \equiv S_n \cdot S_{n-1} \cdot S_{n-1} \qquad (29)$$

where S_n designates the word of the nth periodic orbit arising in the period doubling cascade. Note that the relation (28) is valid for $n > 0$ for the cascade generated by the orbit (1) and for any n for all the other cascades (some of them are reported in table 2). From table 1, one may extract the following relation:

$$slk(\alpha_n) = slk(L_{\alpha_n^R}) + (p_n - q_n). \qquad (30)$$

Also, a recurrence law is found to be obeyed by the self-linking number of the reduced orbit α^R:

$$slk(\alpha_{n+1}^R) = 4slk(\alpha_n^R) + T(L_{\alpha_n}). \qquad (31)$$

Table 2. Effective twist numbers $T(L_\alpha)$ of orbits whose period is less than 8 for a trivial suspension of a horseshoe map. n designates the order of the period-doubling bifurcation in the cascades and p means the topological period of orbits involved in the pair (α_0, β) created by a saddle-node bifurcation where α_0 is the flip saddle and β is the regular saddle.

				$T(L_{\alpha_n})$				
p	Regular	$T(L_\beta)$	Flip	$n=0$	$n=1$	$n=2$	$n=3$	$n=4$
1	(0)	0	(1)	1	3	7	13	27
3	(101)	6	(100)	5	11	21	43	85
4	(1001)	8	(1000)	7	15	29	59	117
5_1	(10111)	8	(10110)	7	15	29	59	117
5_2	(10010)	8	(10011)	9	17	35	69	139
5_3	(10001)	10	(10000)	9	19	37	75	149
6_1	(101110)	6	(101111)	7	13	27	53	107
6_2	(100111)	12	(100110)	11	23	45	91	181
6_3	(100010)	10	(100011)	11	21	43	85	171
6_4	(100001)	12	(100000)	11	23	45	91	181
7_1	(1011111)	14	(1011110)	13	27	53	107	213
7_2	(1011010)	12	(1011011)	13	25	51	101	203
7_3	(1001011)	12	(1001010)	11	23	45	91	181
7_4	(1001110)	12	(1001111)	13	25	51	101	203
7_5	(1001101)	14	(1001100)	13	27	53	107	213
7_6	(1000100)	12	(1000101)	13	25	51	101	203
7_7	(1000111)	14	(1000110)	13	27	53	107	213
7_8	(1000001)	14	(1000000)	13	27	53	107	213

Table 3.

n	0	1	2	3	4	5	6	7	8	9
m type	0	1	1	3	5	11	21	41	83	165
M type	0	1	3	5	11	21	41	83	165	331

Another layer may be proposed to predict the effective twist number $T(L_{\alpha_n})$ with respect to the order n. It reads as

$$T(L_{\alpha_n}) = 2^n \tilde{lk}(L_{\alpha_0}, \alpha_0) + K_n \tag{32}$$

where K_n is a number verifying a Fibonacci series. Again, two classes of period-doubling cascades are distinguished. Indeed, the number K_n may be obtained for $n \geqslant 3$ with seeds $K_1 = 1$ and $K_2 = 1$, when $\tilde{lk}(L_{\alpha_0}, \alpha_0) < \tilde{lk}(L_\beta, \beta)$ and with $K_1 = 1$ and $K_2 = 3$, when $\tilde{lk}(L_{\alpha_0}, \alpha_0) > \tilde{lk}(L_\beta, \beta)$. If we designate the first class of period-doubling cascade being of the minor (m) type and the second one of the major (M) type, the number K_n is then equal to the values shown in table 3.

This table may be obtained from relations (26) and (32).

We conjecture that in the bifucation diagram, M-type and m-type cascades alternatively appear.

5. Conclusion

Topological invariants must be preferred to investigate topological structures rather than other quantities which are not topological invariants such as total twist. As a consequence, a quasi-linking number $\tilde{lk}(L_\alpha, \alpha)$ between the edges L_α of a ribbon whose orbit α is the core and

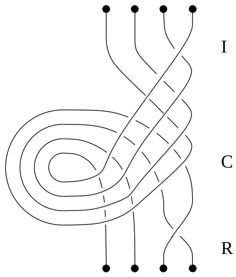

Figure A1. Partially closed braid for the orbit (1011 1010).

this orbit has been introduced to study period-doubling cascades. Of course, this topological invariant may be used to investigate the relative organization of any periodic orbit in any kind of attractor. Its great advantage is that it does not depend on the diagrammatic representation, in contrast with total twists which are often used in investigating period-doubling cascades. When a trivial horseshoe template is considered, quasi-linking numbers $\tilde{lk}(L_\alpha, \alpha)$ may be predicted from the symbolic sequences of orbits. The effective twist number counting the number of half-turns the ribbon locally rotates around its core reduced to its minimal form, may also be predicted with symbolic dynamics but this last result is, however, still of limited significance since the braid index, required for predictions, may, up to now, only be computed from symbolic sequences for trivial horseshoe templates. Nevertheless, the effective twist number provides more information than the total twist number since all dynamical information is preserved under Reidemeister moves.

Acknowledgment

We with to thank Robert Gilmore for much helpful discussions and encouragement.

Appendix A. Explicit relations for period-doubling cascades

The self-linking numbers $slk(\alpha_n)$ and $slk(\alpha_n^R)$ presented in table 1 may indeed be predicted from symbolic dynamics but this has been done with the aid of a computer program for large periodic orbits. In the case of the period-doubling cascade generated by orbit (1) for the horseshoe template of figure 6, it has, however, been possible to rigorously establish, by hand-calculations, analytical expressions for the above self-linking numbers [20]. The demonstration is too lengthy to be provided here but a sketch of it is given below.

Let us consider the braid associated with the period-8 orbit encoded by (1011 1010) given in appendix B ($n = 3$). Instead of reducing it, let us partially close the braid, the closure involving the four leftmost strands (i.e. half of the strands). We then obtain the partially closed braid displayed in figure A1.

This structure exhibits three patterns:

(i) Pattern I. This pattern defines a braid with four strands such that the rightmost point at the top of the braid is connected to the leftmost point at the bottom of the braid, and so on, defining a half-turn applied to the block of strands.
(ii) Pattern C. This patterns exhibits four curls.
(iii) Pattern R. The total braid two generations before (i.e. for $n = 1$).

We established that the pattern of figure A1 occurs at all levels $n > 1$. More specifically, the sub-pattern I exhibits 2^{n-1} strands and the sub-pattern C exhibits 2^{n-1} curls. The self-linking number $slk(\alpha_n)$ is the sum of the number of crossings in each sub-pattern. We then readily obtain

$$slk(\alpha_n) = 2^{n-2}[2^n + 2^{n-1} - 1] + slk(\alpha_{n-2}) \tag{A.1}$$

with initializations

$$\begin{aligned} slk(\alpha_0) &= 0 \\ slk(\alpha_1) &= 1. \end{aligned} \tag{A.2}$$

The recurrence relation (A.1) may also be given a two-step form according to

$$slk(\alpha_n) = 6slk(\alpha_{n-1}) - 8slk(\alpha_{n-2}) + (-1)^m \tag{A.3}$$

with $m = n + 1$ and the same initializations.

These recurrence relations may be explicitly solved, leading to

$$slk(\alpha_n) = \frac{4^{n+1}}{10} - \frac{2^{n+1}}{6} + \frac{(-1)^{n+1}}{15} \qquad (n > 1). \tag{A.4}$$

The partially closed braid may be simplified to a reduced braid by removing the curls. After such a removal, we established that no further simplification is possible. Therefore, we have

$$slk(\alpha_n) - slk(\alpha_n^R) = 2^{n-1} \qquad (n > 0). \tag{A.5}$$

We subsequently establish

$$slk(\alpha_n^R) = 6slk(\alpha_{n-1}^R) - 8slk(\alpha_{n-2}^R) + (-1)^m \tag{A.6}$$

with $m = n + 1$ and the initializations

$$\begin{aligned} slk(\alpha_0^R) &= slk(\alpha_1^R) = 0 \\ slk(\alpha_2^R) &= 3 \end{aligned} \tag{A.7}$$

having the explicit solution

$$slk(\alpha_n^R) = \frac{4^{n+1}}{10} - \frac{5}{12}2^{n+1} + \frac{(-1)^{n+1}}{15} \qquad (n > 1). \tag{A.8}$$

For the cascade starting from the orbit (100), it is empirically found (table 1) that the self-linking number $slk(\alpha_n)$ obeys relation (A.3) with $m = n$ and initializations

$$\begin{aligned} slk(\alpha_0) &= 2 \\ slk(\alpha_1) &= 9 \end{aligned} \tag{A.9}$$

having the explicit solution

$$slk(\alpha_n) = \frac{13}{5}4^n - \frac{2}{3}2^n + \frac{(-1)^n}{15} \qquad (n \geqslant 0). \tag{A.10}$$

Also, $slk(\alpha_n^R)$ obeys relation (A.6) with $m = n$ and the initializations

$$\begin{aligned} slk(\alpha_0^R) &= 0 \\ slk(\alpha_1^R) &= 5 \end{aligned} \tag{A.11}$$

having the explicit solution

$$slk(\alpha_n) = \frac{13}{5}4^n - \frac{8}{3}2^n + \frac{(-1)^n}{15} \qquad (n \geqslant 0). \tag{A.12}$$

Due to the similarity between the relations for the cascade starting from (1) and the cascade starting from (100), we conjecture that equations (A.10)–(A.12) are true. It is likely that they could be established in a way similar to the one used for equations (A.1)–(A.8).

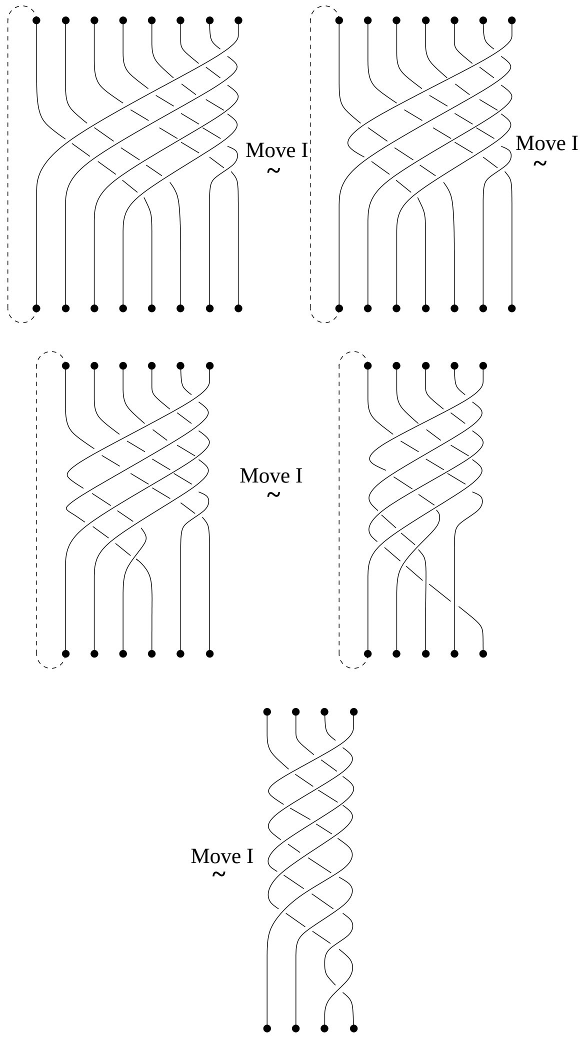

Figure B1. Simplification of the period-8 orbit encoded by (1011 1010). The orbit cannot be reduced to the trivial knot. Its braid index is equal to four as predicted by the decomposition in syllables reading as 011 · 1 · 01 · 01.

Appendix B. Simplification of the period-8 orbit

In figure B1 we show the period-8 orbit encoded by (1011 1010).

References

[1] Birman J and Williams R F 1983 *Topology* **22** 47–82
[2] Birman J and Williams R F 1983 *Cont. Math.* **20** 1–60
[3] Mindlin G B, Hou X J, Solari H G, Gilmore R and Tufillaro N B 1990 *Phys. Rev. Lett.* **64** 2350
[4] Mindlin G B and Gilmore R 1992 *Physica* D **58** 229
[5] Tufillaro N B, Abbott T and Reilly J 1992 *An Experimental Approach to Non Linear Dynamics and Chaos* (New York: Addison-Wesley)
[6] Letellier C, Dutertre P and Maheu B 1995 *Chaos* **5** 271

[7] Uezu T 1983 *Phys. Lett.* A **93** 161
[8] Solari H G and Gilmore R 1988 *Phys. Rev.* A **37** 3096
[9] Beiersdorfer P, Wersinger J and Treve Y 1983 *Phys. Lett.* A **96** 269
[10] Crawford J D and Omohundro S 1984 *Physica* D **13** 161
[11] Gonzales D L, Magnasco M O, Mindlin G B, Larrondo H A and Romanelli L 1989 *Physica* D **39** 111
[12] Bergé P, Pomeau Y and Vidal C 1984 *L'Ordre Dans Le Chaos* (Paris: Hermann)
[13] Kauffman L H 1987 *On Knots* (Princeton, NJ: Princeton University Press)
[14] Cãlugãreanu G 1959 *Rev. Math. Pures Appl.* **4** 5
[15] Moffatt H K and Ricca R L 1992 *Proc. R. Soc.* A **439** 411
[16] Melvin P and Tufillaro N B 1991 *Phys. Rev.* A **44** 3419
[17] Le Sceller L, Letellier L and Gouesbet G 1994 *Phys. Rev.* E **49** 4693
[18] Alexander J W 1923 *Proc. Natl Acad. Sci., USA* **9** 93
[19] Ghrist R and Holmes P 1993 Knots and orbits genealogies in three dimensional flows *Bifurcations and Periodic Orbits of Vector Fields* (Netherlands: Kluwer) p 185
[20] Gouesbet G 1998 Knot and knot in variant structures in a period-doubling cascade (Internal report available upon request)